RSC Advances

ROYAL SOCIETY OF CHEMISTRY

www.rsc.org/advances

Enhanced visible photocatalytic activity of Cu_2O nanocrystal/titanate nanobelt heterojunctions by self-assembly process

Yueli Liu, Guojie Yang, Hao Zhang, Yuqing Cheng, Keqiang Chen, Zhuoyin Peng, Wen Chen*

* To whom correspondence should be addressed:

[*] State Key Laboratory of Advanced Technology for Materials Synthesis and Processing, School of Materials Science and Engineering, Wuhan University of Technology, Wuhan, 430070 (P. R. China)

Tel.: +86-27-8765-1107

Fax: +86-27-8776-0129

E-mail: **chenw@whut.edu.cn (Wen Chen)**

Abstract

In the present work, we introduce a facile and widely-used route to fabricate Cu_2O nanocrystal/titanate nanobelt heterojunctions with high yield, well dispersion and tight interaction, which are self-assembled via the linker molecule of 3-Mercaptopropionic acid. Their photocatalytic activity for the degradation of methyl orange solution will be enhanced by the decorating with Cu_2O nanocrystals, especially in visible light region. The degradation ratio of 6 wt% Cu_2O/titanate heterojunctions is the best one of 100%, while that of the pure titanate nanobelts.is of only 20% and 3%, respectively, after 80 and 180 minutes' irradiation under the UV and visible light irradiation. As the p-n heterojunctions will suppress the recombination of electron-hole pairs in titanate nanobelts, where the Cu_2O nanocrystals act as electron traps aiding electron-hole separation, moreover, a synergistic effect of the tight contact between Cu_2O nanocrystals and titanate nanobelts also favors for the efficiently enhancement of photodegradation rate of the Cu_2O/titanate heterojunctions.

Keywords: Cu_2O nanocrystal/titanate nanobelt heterojunctions; self-assembly; linker molecules; photocatalytic activity

1. Introduction

Currently, many semiconductor photocatalysts have been paid more attention to solve the environmental pollution, and how to make full use of the light energy is the key factor for the efficient and mild route to photodegrade the wastes. [1-5] Among

them, titanate nanomaterials are of great interest for photocatalysis since they possess a good photocatalytic activity. [6-8] However, the titanate nanomaterials with wide band gap (about 3.0 eV) only absorb a small fraction of solar light, and thus limit their efficient photocatalytic performance in visible light.

As a p-type semiconductor, Cu_2O possesses a direct band gap of 2.0 eV and a high optical absorption coefficient, and it is considered to be a prospective candidate in the visible photocatalysis application. [9] However, its photocatalytic performance is limited by the recombination of the photogenerated electron and hole. [10-11] Due to the matching of the band structure between Cu_2O and titanate, the forming of the p-n junction is an effective way to solve their above problems and to improve their photocatalytic performance in visible light. [12-15]

Recently, Cu_2O/TiO_2 p–n heterojunction photoelectrodes were prepared via an ultrasonication-assisted sequential chemical bath deposition, which possessed superior photoelectrocatalytic activity and stability in the degradation of Rhodamine B. [16] Ultra-small Cu_2O nanoparticles were loaded on TiO_2 nanosheets with {001} facets exposed through a one-pot hydrothermal reaction, and its excellent visible-light activity was about 3 times of N-doped TiO_2 nanosheets exposed with {001} facets. [17] Cu_2O/TiO_2 nanobelt heterostructures were prepared by the wet precipitation method, which displayed much higher adsorbability than pure TiO_2 nanobelts, while it was difficult to control the interface combination between Cu_2O nanocrystals and TiO_2 nanobelts. [18] Lalitha et al. prepared Cu_2O/TiO_2 naocomposites and found that it could photogenerate H_2 from glycerol and water mixtures under visible light irradiation. [19] Huang et al. prepared a heterostructure of TiO_2 and smaller Cu_2O nanoparticles (2–3 nm) through an alcohol-aqueous based chemical precipitation method, [20] and it exhibited much better efficiency than P25 on degradation of acid orange both under

visible and UV-Vis lights irradiation.

However, the key problem remains the difficulty of controlling the metal particle size, dispersion, and composition, etc, especially for the combination between the various semiconductor materials till now, as it will influence the effective separation of the photo-excited electrons and holes, which is able to suppress their direct recombination. [21-25] In our previous work, Pt(Au) nanocrystals [7-8] and $CuInS_2$ quantum dots [26-29] are combined with titanate nanobelts by the bifunctional molecules, which may form a good interface combination.

Following this easy process, Cu_2O nanocrystal/titanate nanobelt heterojunctions are self-assembled with high yield, well dispersion and tight interaction, and it is expected to possess an enhanced photocatalytic activity towards methyl orange solution under visible light irradiation.

2. Experimental

2.1. Synthesis of 1-D titanate nanobelts and Cu_2O nanocrystals

The 1-D titanate nanobelts were synthesized according to our previous work. [6-8]

Cu_2O nanocrystals were synthesized by a modified hydrothermal method: 0.06 mol of cuppric acetate was added into 600 mL of deionized water, and then 3.6 mL of PEG-400 was added into the solution with vigorous stirring. Then, a mixture of NaOH and hydrazine with volume ratio of 1/3 was dropped into the solution, and then the solution was transferred into an autoclave. The autoclave was sealed and maintained at 180 ºC for 8 h and then cooled down to room temperature. A red brown precipitate was washed several times with distilled water and dried at room temperature. The samples were added to the methanol solution of MPA, and the MPA-capped Cu_2O nanocrystals were prepared for use in the next step. The Cu_2O contents are controlled by the different concentration of Cu_2O nanocrystals, for

simplify, the samples are signed as (x wt%) Cu_2O/titanate.

2.2. Self-assembly process

In the experiment, 3-Mercaptopropionic acid (MPA) purchased from Sigma-Aldrich was used as a linker molecule. The prepared titanate nanobelts were heating dried at 100 ℃ for 5 h to remove H_2O molecules from the surface due to the ambient humidity adsorption. They were put into the methanol solution of MPA overnight in nitrogen protected environment in glovebox, and cleaned by toluene solvent for several times to remove the extra MPA solvent, and then the carboxylate group binds tightly with titanate nanobelts. The MPA-treated titanate nanobelt powders (0.4 g) were dispersed in the solution of MPA-capped Cu_2O nanocrystals, following by the sonication for 2 h at room temperature. The final products were separated and washed by toluene and ethanol solvents in order with centrifugation, then dried in an oven at 100 °C, and finally they were annealed at 300 °C for 2h in air to remove the organic molecules.

2.3. Photocatalytic activity experiments

Before the irradiation, 0.05 g (x wt%) Cu_2O/titanate heterojunctions were put into aqueous methyl orange solution (50 mL, 32.73 ppm), and then the suspension is stirred for 2 h in the dark environment to achieve the establishment of an adsorption/desorption equilibrium. Photogradation rate of Cu_2O/titanate heterojunctions was evaluated by examining the concentration variation of methyl orange under UV and visible light illumination from the light source of 125 W high-pressure Hg lamps for every 60 min, respectively, which has UV (200-400 nm) and visible light (400-800 nm) spectra with the main peak located at the 365 nm wavelength. For the visible light irradiation, the light source is equipped with an UV cutoff filter, which may remove 99% of UV light with the wavelength between 320

nm and 400 nm. The irradiation light intensity on the samples under UV and visible light illumination was kept equally by adjusting the distance between the lamp and samples, respectively.

2.4. Characterization

The morphologies and microstructures of the samples are characterized by using scanning electron microscope (SEM) (Zeiss Ultra-55, ZEISS, German), regular transmission electron microscope (TEM) (JEM2100FEF, JEOL, Japan), X-ray diffractometer (XRD) (PertPro, PANalytical, The Netherlands), and UV-Vis spectra are tested using UV-2550 spectrophotometer. X-ray photoelectron spectroscopy (XPS) measurement was performed in the Escalabmk-Ⅱ XPS apparatus (VG Scientific, England) with Al target. The emission angle between the photoelectron beam and the sample surface was 45°, and the calibration of the binding energy of the electron spectrometer was made by using the maximum adventitious C1s signal at 284.6 eV with the solution of the full width at half maximum (FWHM) being 0.8 eV.

3. Results and discussion

The typical SEM image of the titanate nanobelts in Fig. 1(a) shows a lot of homogeneous structures existing with their width of about 70~80 nm and the length of several micrometers. Their crystal structure is also evaluated by the XRD patterns in Fig. 1(b), which contains the diffraction peak at 2θ value of 8.9°, and this characteristic peak implies that the nanobelts are composed of a layered titanate structure of $H_2Ti_5O_{11}\cdot 3H_2O$ phase (JCPDS No.: 44-0130) . [6-8] After decorating with Cu_2O nanocrystals, the diffraction peaks at 29.9°, 35.6°, 53.1° and 61.4° correspond to the (110), (111), (211) and (220) planes of the cubic Cu_2O phase (JCPDS No.: 78-2076), which indicates that the formation of Cu_2O phase in the Cu_2O/titanate heterojunctions. [16-20]

Fig. 2 shows the SEM images of the Cu_2O/titanate heterojunctions at various Cu_2O contents, and the Cu_2O nanocrystals with the diameters of 7-9 nm are well dispersed on the surface of titanate nanobelts by the effect of the MPA coupling agent. It is worth to mention that the deposition contents of Cu_2O nanocrystals increase with the increasing of the contents of Cu_2O/titanate heterojunctions, which actually matches with the XRD patterns in Fig. 1(b). For example, in Fig. 2(a) there are only a few Cu_2O nanocrystals dispersed on the surface of the titanate nanobelts, while there are many Cu_2O nanocrystals dispersed on the surface of the titanate nanobelts with the increasing of the deposition contents of Cu_2O nanocrystals especially for the sample of 8 wt% Cu_2O/titanate heterojunction. The linking process of the Cu_2O nanocrystals will further influence the optical and photocatalytic properties of the Cu_2O/titanate heterojunction. As Ti-O-Ti bonds have a strong affinity for the carboxylate group of the linker molecules, while the sulfur atom of MPA binds strongly to Cu_2O atom via the S-metal junction. [30-31] Therefore, Cu_2O nanocrystals bind with the titanate nanobelts through the function of MPA molecules, similar with that of the Pt(Au)/titanate [7-8] and $CuInS_2$/titanate heterojunctions. [26-29]

It is well known that the photocatalytic activity of Cu_2O nanocrystals is related with their sizes and phases as well as their chemical binding states. [32-33] The XPS survey spectra in Fig. 3(a) show that Cu, Ti and O elements coexist. Cu 2*p* spectrum in Fig. 3(b) shows the characteristic of the substance Cu^1 phase with $2p_{1/2}$ peak located at 953.2 eV. Ti 2*p* spectra in Fig. 3(c) illustrate the existence of Ti^{4+} ions with $2p_{1/2}$ peak located at about 463.90 eV, and it is located in 463.86 eV after the deposition of Cu_2O nanocrystals. O 1*s* spectra in Fig. 3(d) show that two chemical states of oxygen coexist, and the peak located at 530.14 eV belongs to the O^{2-} in the Ti-O-Ti and Cu-O binding formation of titanate nanobelts and Cu_2O nanocrystals,

respectively, while the peak located at 531.97 eV proves the existence of surface-adsorbed hydroxide (OH), [33] which is physically adsorbed on the surface due to their unique belt-like structure and high ratio between the length to diameter. From the spectra, there is no obvious peak shift of O 1*s* peak after the deposition of Cu_2O nanocrystals, however, the relative intensity of the peaks of 530.14 eV to peak of 531.97 eV increases from 1:2.58 to 1:1.21, which partially originates from the deposition of Cu_2O nanocrystals as well as the increasing of the surface-adsorbed hydroxide. It is well known that the adsorbed hydroxide species are quite important for the process of photocatalytic reaction, [34-35] as it may produce hydroxyl radical (·OH) by capturing the photo-induced electrons, which favors for the oxidizing of the organic materials and the oxidizing hydroxylating reaction products as the oxidant. [36] Therefore, the increase of the hydroxide absorption in Cu_2O/titanate heterojunctions will favor for their photocatalytic reaction, as the physical absorption ability of hydroxide species not only enhances the separation efficiency of photo-induced electrons and holes, but also promotes the transfer of photo-induced electrons to the adsorbed hydroxide species.

UV-Vis spectra are used to character the optical absorption of all of the above samples in the wavelength range of 300-800 nm in Fig. 4. It shows that the Cu_2O/titanate heterojunctions possess an obvious enhanced UV and visible light absorption comparing with titanate nanobelts, however, the visible light absorption of the all Cu_2O/titanate heterojunctions is not higher than that of the pure Cu_2O nanocrystals. For all of the Cu_2O/titanate heterojunctions, the 6 wt% Cu_2O/titanate heterojunction achieve the highest optical absorption intensity. The reason lies in the fact that the concentration of oxygen vacancies capturing electron formed during the synthesis process has an important effect on the light absorption, [37-38] and the

formation of the heterojunctions might favor for the stability of the oxygen vacancies. Moreover, considering the band gap of the 6 wt% Cu_2O/titanate heterojunctions, it shifts to be 2.57 eV if comparing with that of the Cu_2O nanoparticles (2.0 eV) and titanate nanobelts (3.0 eV) [6]. Therefore, some energy levels may be produced in the band gap of titanate nanobelts by the dispersion of Cu_2O nanocrystals on the surface of the titanate nanobelts, which may lead to the phenomenon that the optical absorption enhances significantly.

The catalytic efficiency of the various Cu_2O/titanate heterojunctions is evaluated in terms of the degradation rate of methylene orange (MO) under UV light and visible light irradiation, respectively. The ratio of the intensity of the MO's absorption bands before and after irradiation (I/I_0) is correlated with irradiation time in Fig. 5 by choosing the absorption peak at 586 nm. To show the confidence level of the photocatalytic performance of the samples, we have carried out two independent sets of the photodegradation experiments, which are used to show the error bar in all of the cures in Fig. 5. It shows that the photodegradation rates of the pure titanate nanobelts and Cu_2O nanoparticles are about 20% and 73% after 80 minutes' UV light irradiation, respectively, and that of 6 wt% Cu_2O/titanate heterojunction has the best photodegradation efficiency and may totally photodegrade the MO molecules as shown in Fig. 5(a).

The photodegradation rate of the pure titanate nanobelts is only 3% and 5% after 180 and 300 minutes' visible light irradiation, respectively, and the one of the and Cu_2O nanoparticles after 180 minutes' visible light irradiation is about 81%, while 6 wt% Cu_2O/titanate heterojunction has the best photodegradation efficiency and may totally photodegrade the MO molecules after 180 minutes' visible light irradiation as shown in Fig. 5(b). It shows that the reaction rate increases than that of the pure

titanate nanobelts by a factor of 5 under UV-light irradiation, and even a factor of 34 under visible-light irradiation, which is quite good comparing with the others' similar reports. [20-21] Therefore, the Cu_2O nanocrystals deposited on the surface of titanate nanobelts can efficiently enhance the photodegradation ability, which results from the fact that the titanate nanobelts may accelerate the separation of photogenerated electrons and hole on Cu_2O nanocrystals in the heterojunctions, as in visible light region, Cu_2O nanocrystals are the main active species. [20] On the other hand, the excess loading of Cu_2O nanocrystals (8 wt%) will decrease the optical absorption over some certain value due to the shading effect, [8, 39] and then decreases the photocatalytic properties, and it is in consistent with UV-Vis spectra in Fig. 4.

The photocatalytic performances of pure titanate nanbelts, Cu_2O nanocrystals and 6 wt% Cu_2O/titanate heterojunction have been investigated in two cycles to check the photocatalytic stability under 80 mins' UV and 180 mins' visible light irradiation, as shown in Fig. 6. It is shown that the activity of 6 wt% Cu_2O/titanate heterojunction decreases slightly in 1st reuse and kept stable in the next cycle. However, for pure titanate nanbelts, Cu_2O nanocrystals, especially for the pure Cu_2O nanocrystals, the activities decreased gradually from 73% and 85% for fresh catalyst to 55% and 64.8% for 2nd reused catalyst under 80 mins' UV and 180 mins' visible light irradiation, separately. The fact implies that the photocatalytic stability of 6 wt% Cu_2O/titanate heterojunction is much better than that of the pure titanate nanbelts and Cu_2O nanocrystals, which implies that the potential application in the UV and Vis photodegradation.

It is well known that a typical p-n junction barrier at the interface between Cu_2O nanocrystals and semiconductor titanate nanobelts will be formed, [20-21] as the heterojunctions will suppress the recombination of electron-hole pairs in titanate

nanobelts, where the Cu_2O nanocrystals act as an efficient electron traps aiding electron-hole separation. The possible mechanism of the heterojunctions can be understood through the energy band diagram of the heterojunctions as shown in Fig. 7. In UV region, both of the Cu_2O nanocrystals and titanate nanobelts may be photoexcited to generate electrons under irradiation from the valence band (VB) to the conduction band (CB), which may migrate to the surface of the heterojunctions. The p-n junction barrier facilitates the electron capture, and it will increase the lifetime of the photo-excited electron-hole pairs and retards the electron-hole recombination to enhance the photocatalytic performance. Then the photo-excited electrons migrate to O_2 molecules adsorbed on the surface of Cu_2O nanocrystals, [39] and subsequently reduce the recombination between electrons and holes, allowing more opportunities for the electrons to participate in the reduction reaction to form superoxide radicals (O_2^-), which serves as a strong oxidant that can decompose MO molecules effectively. At the same time, the holes created under irradiation on titanate nanobelts participate in the oxidation reaction to produce hydroxyl radicals (·OH), which is a very strong oxidant to favor for the decomposition of organic substances in parallel.

Meanwhile, in visible light region, most of the photoexcited electrons are generated due to the narrow band gap of Cu_2O nanocrystals (2.0 eV), which may diffuse through the Cu_2O/titanate interface into CB of titanate nanobelts. Moreover, the position of CB of Cu_2O nanocrystals is considered to be above the CB of titanate nanobelts, [20] which may favor for the migration of the photo-excited electrons and then acceleration of the production of superoxide and hydroxyl radicals.

4. Conclusions

Cu_2O nanocrystal/titanate nanobelt heterojunctions are self-assembled with the linker molecule of 3-Mercaptopropionic acid. After 80 and 180 minutes' irradiation

under the UV and visible light irradiation, the photodegradation efficiency of the pure titanate nanobelts is only 20% and 3%, respectively, while 6 wt% Cu_2O/titanate heterojunction has the best photodegradation efficiency and may totally photodegrade the MO molecules. Therefore, the present work will provide a novel route to greatly enhance the photocatalytic properties of Cu_2O/titanate heterojunctions, especially in visible light region.

Acknowledgements

This work is supported by the International S&T Cooperation program of China (ISTCP) ((No. 2013DFR50710), the National Nature Science Foundation of China (No. 50802070) and the Fundamental Research Funds for the Central Universities (2012-□-007).

References

[1] J. Zhang, J. H. Xi and Z. G. Ji, *J. Mater. Chem.*, 2012, **22**, 17700.

[2] H. Zhang, D. Y. Tang, L. M. Zhao, Q. L. Bao and K. P. Loh, *Appl. Phys. Lett.*, 2010, **96**, 111112.

[3] J. Zhang, Y. P. Zhang, Y. K. Lei and C. X. Pan, *Catal. Sci. Technol.*, 2011, **1**, 273.

[4] Z. W. Zheng, C. J. Zhao, S. B Lu, Y. Chen, Y. Li, H. Zhang and S. C. Wen, *Opt. Express*, 2012, **20**, 23201.

[5] J. Zhang, W. Fu, J. H. Xi, H. He, S. C. Zhao, H. W. Lu and Z. G. Ji, *J. Alloys Comp.*, 2013, **575**,40.

[6] Y. L. Liu, W. Shu, K. Q. Chen, Z. Y. Peng and W. Chen, *ACS Catal.*, 2012, **2**, 2557.

[7] Y. L. Liu, L. Zhong, Z. Y. Peng, Y. Cai, Y. H. Song and W. Chen, *CrystEngComm*, 2011, **13**, 5467.

[8] Y. L. Liu, W. Shu, Z. Y. Peng, K. Q. Chen and W. Chen, *Catal. Today*, 2013, **208**, 28.

[9] S. D. Sun, X. P. Song, Y. X. Sun, D. C. Deng and Z. M. Yang, *Catal. Sci. Technol.*, 2012, **2**, 925.

[10] J. Zhang, W. K. Chen, J. H. Xi and Z. G. Ji, *Mater. Lett.*, 2012, **79**, 259.

[11] R. Prasad and P. Singh, *Catal. Sci. Technol.*, 2013, **3**, 3326.

[12] J. Zhang, G. Ma, H. H. Zhu, J. H. Xi and Z. G. Ji, *J. Anal. Atom. Spectrom.*, 2012, **27**, 1903.

[13] Q. L. Bao, H. Zhang, B. Wang, Z. H. Ni, C. Haley, Y. X. Lim, D. Y. Tang and K. P. Loh, *Nat. Photonics*, 2011, **5**, 411.

[14] S. S. Zhang, S. Q. Zhang, F. Peng, H. M. Zhang, H. W. Liu and H. J. Zhao, *Eletrochem. Comm.*, 2011, **13**, 861.

[15] C. S. Dong, M. L. Zhong, T. Huang, M. X. Ma, D. Wortmann, M. Brajdic and I. Kelbassa, *ACS Appl. Mater. Interf.*, 2011, **3**, 4332.

[16] M. Y. Wang, L. Sun, Z. Q. Lin, J. H. Cai, K. P. Xie and C. J. Lin, *Energy*

Environ. Sci., 2013, **6**, 1211.

[17] L. C. Liu, X. R. Gu, C. Z. Sun, H. Li, Y. Deng, F. Gao and L. Dong, *Nanoscale*, 2012, **4**, 6351.

[18] J. Zhang, W. Liu, X. Wang and B. Hu, *Appl. Surf. Sci.*, 2013, **282**, 84.

[19] Lalitha, G. Sadanandam, V. D. Kumari, M. Subrahmanyam and B. Sreedhar, *J. Phys. Chem. C*, 2010, **114**, 22181.

[20] L. Huang, F. Peng, H. Wang, H. Yu and Z. Li, *Cataly. Comm.*, 2009, **10**, 1839.

[21] A. Talebian, M. H. Entezari and N. Ghows, *Chem. Eng. J.*, 2013, **229**, 304.

[22] Z. W. Zheng, C. J. Zhao, S. B. Lu, Y. Chen, Y. Li, H. Zhang and S. C. Wen, *Opt. Express*, 2012, **20**, 23201.

[23] H. Matsui, Y. Saitou, S. Karuppuchay, M. A. Hassan and M. Yoshihara, *J. Alloys Comp.*, 2012, **538**, 177.

[24] Y. Wang, K. Yu, H. H. Yin, C. Q. Song, Z. L. Zhang, S. C. Li, H. Shi, Q. F. Zhang, B. Zhao, Y. F. Zhang and Z. Q. Zhu, *J. Phys. D.: Appl. Phys.*, 2013, **46**, 75303.

[25] H. Zhang, S. Virally, Q. L. Bao, K. P. Loh, S. Massar, N. Godbout and P. Kockaert, *Opt. Lett.*, 2012, **37**, 1856.

[26] Z. Y. Peng, Y. L. Liu, Y. H Zhao, W. Shu, K. Q. Chen and W. Chen, *Electrochim. Acta*, 2013, **111**, 755.

[27] Z. Y. Peng, Y. L. Liu, W. Shu, K. Q. Chen and W. Chen, *Chem. Phys. Lett.*, 2013, **586**, 85.

[28] Z. Y. Peng, Y. L. Liu, W. Shu, K. Q. Chen and W. Chen, *Eur. J. Inorg. Chem.*, 2012, **32**, 5239.

[29] Z. Y. Peng, Y. L. Liu, K. Q. Chen, G. J. Yang and W. Chen, *Chem. Eng. J.*, 2014, **244**, 335.

[30] T. López Luke, A. Wolcott, L. P. Xu, S. W. Chen, Z. H. Wen, J. H. Li, E. De La Rosa and J. Z. Zhang, *J. Phys. Chem. C*, 2008, **112**, 1282.

[31] I. Mora Seró, S. Giménez, T. Moehl, F. Fabregat Santiago, T. Lana Villareal, R. Gómez and J. Bisquert, *Nanotech.*, 2008, **19**, 424007.

[32] Y. C. Pu, Y. C. Chen and Y. J. Hsu, *Appl. Catal. B*, 2010, **97**, 389.

[33] M. A. Fox and M. T. Dulay, *Chem. Rev.*, 1993, **93**, 341.

[34] R. Ma, T. Sasaki and Y. Bando, *J. Am. Chem. Soc.*, 2004, **126**, 10382.

[35] M. R. Hoffmann, S. T. Martin, W. Y. Choi and D. W. Bahnemann, *Chem. Rev.*, 1995, **95**, 69.

[36] A. Nakahira, T. Kubo, Y. Yamasaki, T. Suzuki and Y. Ikuhara, *Jpn. J. Appl. Phys.*, 2005, **44**, L690.

[37] J. J. Yi, P.Yu and X. X. Xu, *Acta Polym. Sin.*, 2001, **3**, 342.

[38] S. L. Zhang, W. Li, Z. S. Jin, Z. J. Zhang and Z. L. Du, *J. Solid State Chem.*, 2004, **177**, 1365.

[39] F. B. Li and X. Z Li, *Chemosphere*, 2002, **48**, 1103.

Figure captions

Fig. 1 Microstructures observation of the samples: (a) SEM image of titanate nanobelts; (b) XRD patterns of titanate nanobelts and various Cu_2O/titanate heterojunctions

Fig. 2 SEM images of the Cu_2O/titanate heterojunctions with various Cu_2O contents: (a) 2 wt%; (b) 4 wt%; (c) 6 wt%; (d) 8 wt%

Fig. 3 XPS observations of 1-D titanate nanobelts and 6 wt% Cu_2O/titanate heterojunctions: (a) survey spectrum; (b) Cu 2*p* spectrum; (c) Ti 2*p* spectra; (d) O 1*s* spectra

Fig. 4 UV-Vis spectra of the various Cu_2O/titanate heterojunctions

Fig. 5 Photodegradation curves of 1-D titanate nanobelts and Cu_2O/titanate heterojunctions: (a) under UV light irradiation; (b) under visible light irradiation

Fig. 6 Photodegradation stability of pure titanate nanobelts, Cu2O nanocrystals and 6 wt% Cu_2O/titanate heterojunctions: (a) under 80 mins' UV light irradiation; (b) under 180 mins' visible light irradiation

Fig. 7 Energy band diagram of Cu_2O/titanate heterojunctions

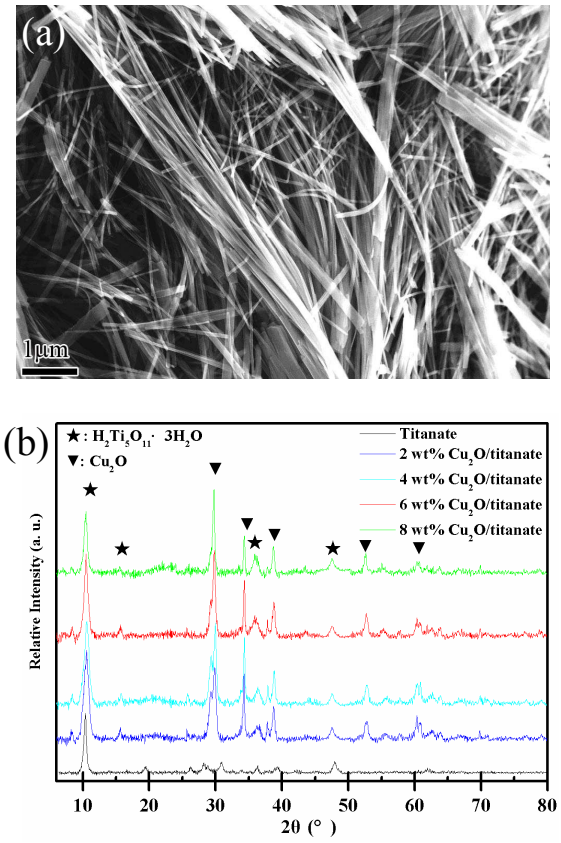

Fig. 1 Microstructures observation of the samples: (a) SEM image of titanate nanobelts; (b) XRD patterns of titanate nanobelts and various Cu_2O/titanate heterojunctions

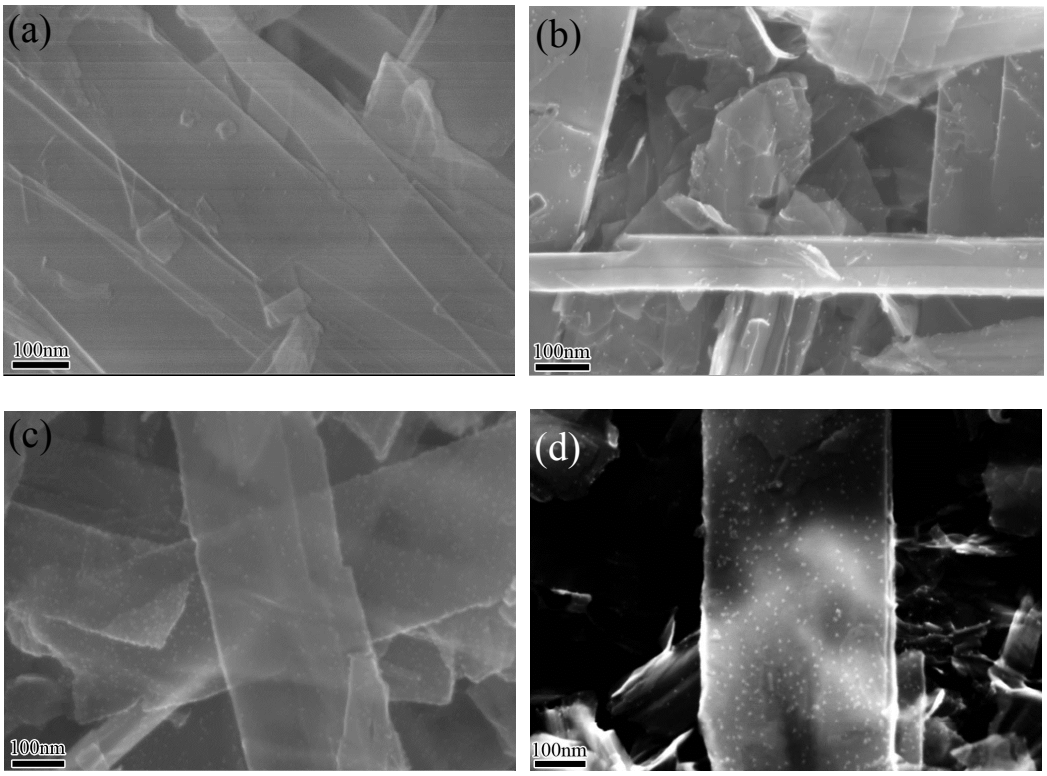

Fig. 2 SEM images of the Cu_2O/titanate heterojunctions with various Cu_2O contents: (a) 2 wt%; (b) 4 wt%; (c) 6 wt%; (d) 8 wt%

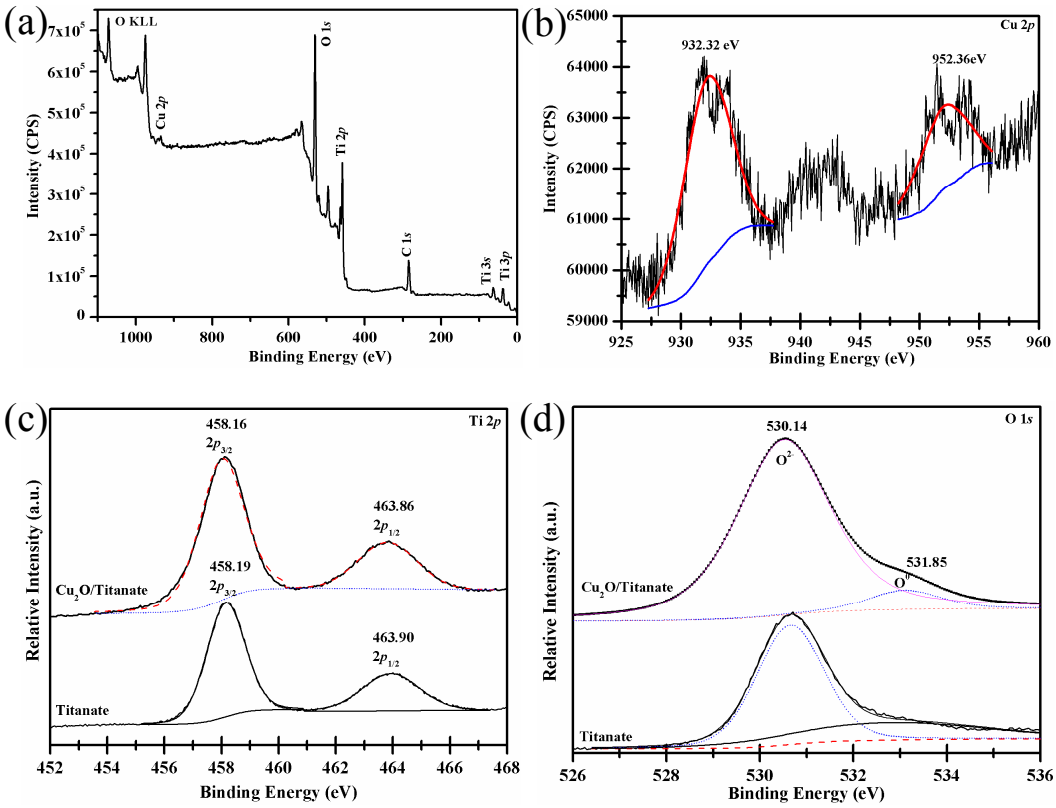

Fig. 3 XPS observations of 1-D titanate nanobelts and 6 wt% Cu_2O/titanate heterojunctions: (a) survey spectrum; (b) Cu 2*p* spectrum; (c) Ti 2*p* spectra; (d) O 1*s* spectra

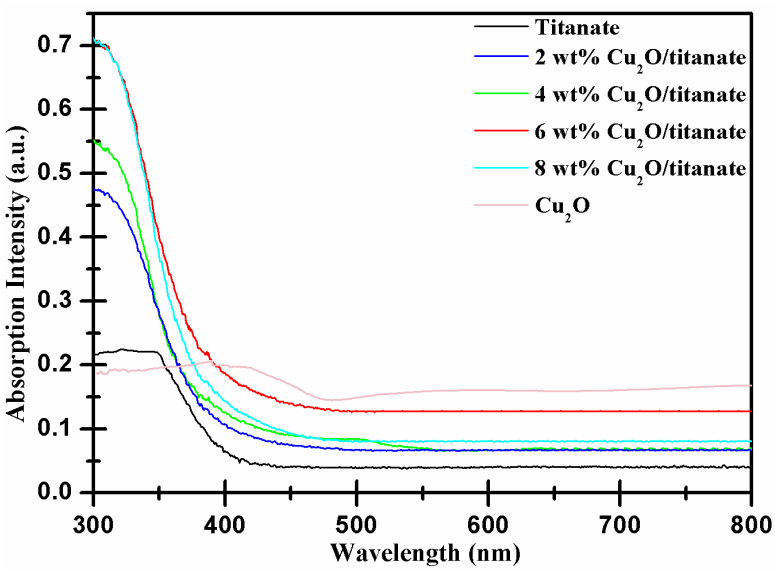

Fig. 4 UV-Vis spectra of the various Cu_2O/titanate heterojunctions

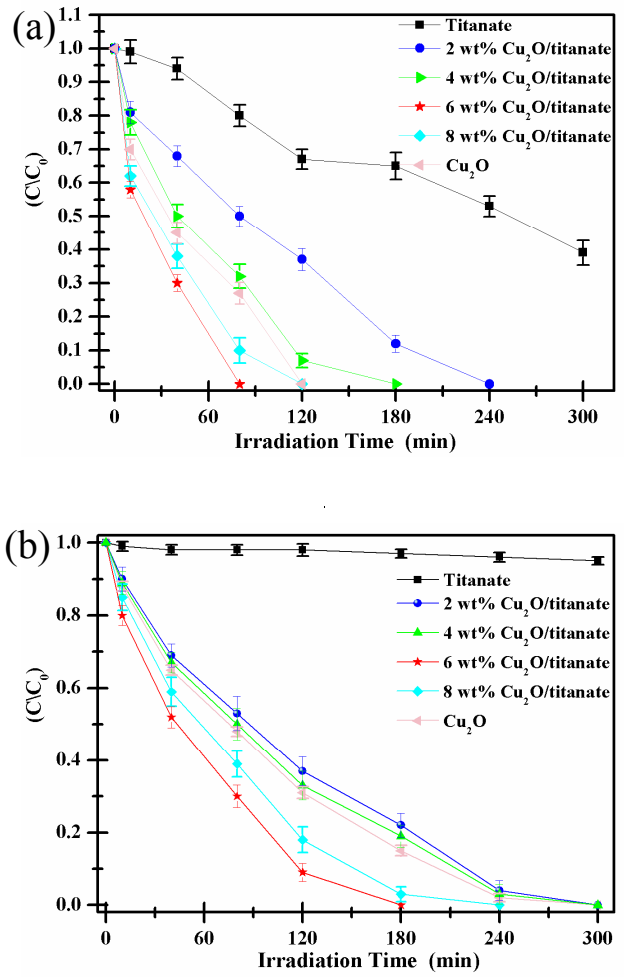

Fig. 5 Photodegradation curves of 1-D titanate nanobelts and Cu_2O/titanate heterojunctions: (a) under UV light irradiation; (b) under visible light irradiation

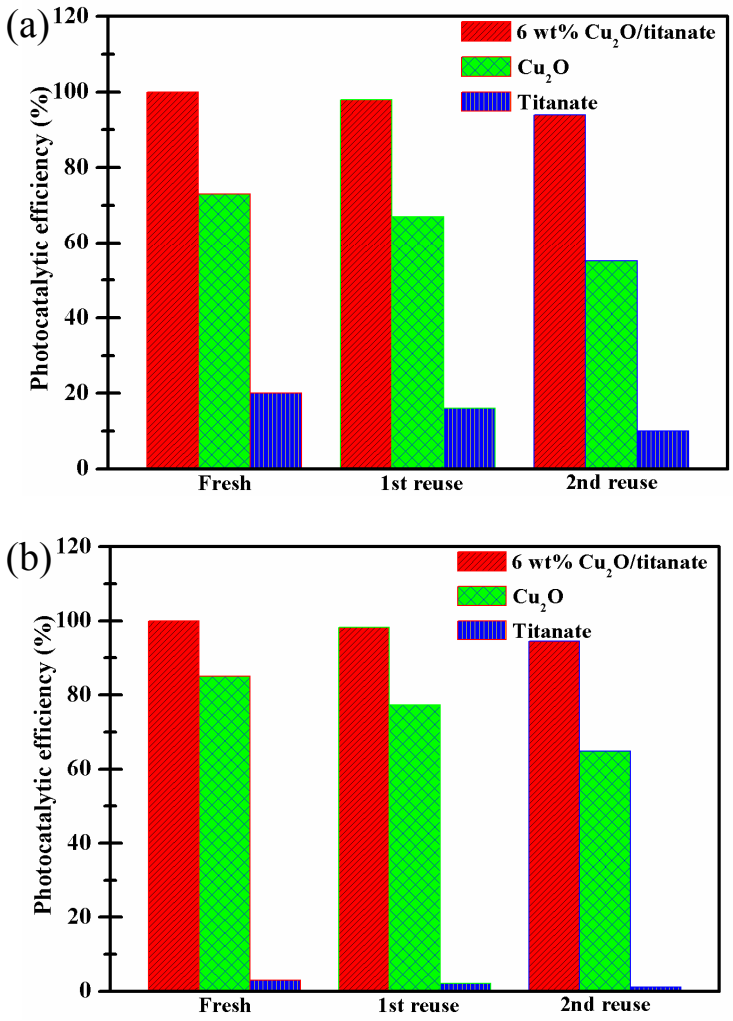

Fig. 6 Photodegradation stability of pure titanate nanobelts, Cu2O nanocrystals and 6 wt% Cu_2O/titanate heterojunctions: (a) under 80 mins' UV light irradiation; (b) under 180 mins' visible light irradiation

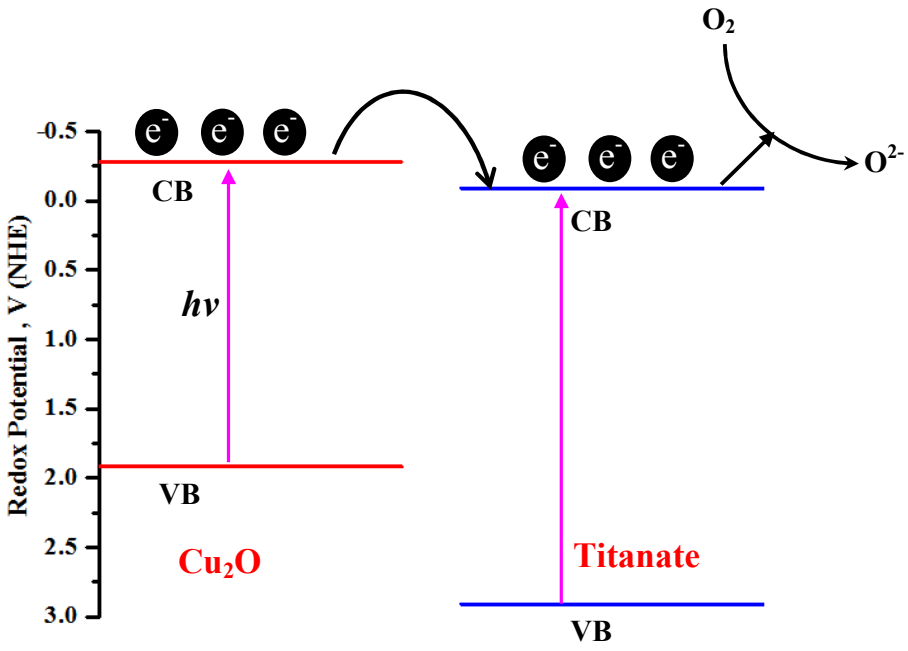

Fig. 7 Energy band diagram of Cu_2O/titanate heterojunctions

Graphical abstract

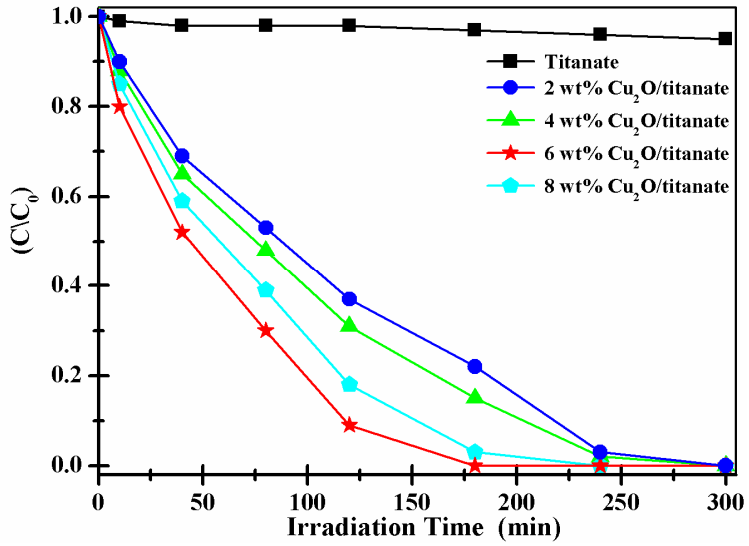

Photodegradation curves of Cu_2O/titanate heterojunctions under visible light irradiation